BnIR: a multi-omics database with various tools for *Brassica napus* research and breeding

Zhiquan Yang[1,2,3,†], Shengbo Wang[1,2,†], Lulu Wei[1,2], Yiming Huang[1,2], Dongxu Liu[1,2], Yupeng Jia[1,2], Chengfang Luo[1,2], Yuchen Lin[1,2], Congyuan Liang[1,2], Yue Hu[1,2], Cheng Dai[1], Liang Guo[1], Yongming Zhou[1], Qing-Yong Yang[1,2,*]

[1]National Key Laboratory of Crop Genetic Improvement, Hubei Hongshan Laboratory, Huazhong Agricultural University, Wuhan, 430070, China

[2]Hubei Key Laboratory of Agricultural Bioinformatics, College of Informatics, Huazhong Agricultural University, Wuhan, 430070, China

[3]Innovative Center of Molecular Genetics and Evolution, School of Life Sciences, Guangzhou University, Guangzhou, 510405, China

[†]These authors contributed equally: Zhiquan Yang, Shengbo Wang.

[*]Correspondence: Qing-Yong Yang (email: yqy@mail.hzau.edu.cn)

Short Summary

In this study, we developed BnIR (http://yanglab.hzau.edu.cn/BnIR), a multi-omics database for rapeseed that integrates six omics datasets and "variation-gene expression-phenotype" associations. The database is equipped with a range of multi-omics tools for streamlined browsing and analysis. Through multiple case studies, we demonstrated BnIR's potential to identify candidate genes associated with specific traits and investigate their regulatory mechanisms.

Abstract

In the post-GWAS era, multi-omics techniques have shown great power and potential for candidate gene mining and functional genomics research. However, due to the lack of effective data integration and multi-omics analysis platforms, such techniques have not still been applied widely in rapeseed, an important oil crop worldwide. Here, we constructed a rapeseed multi-omics database (BnIR; http://yanglab.hzau.edu.cn/BnIR), which provides datasets of six omics including genomics, transcriptomics, variomics, epigenetics, phenomics and metabolomics, as well as numerous "variation-gene expression-phenotype" associations by using multiple statistical methods. In addition, a series of multi-omics search and analysis tools are integrated to facilitate the browsing and application of these datasets. BnIR is the most comprehensive multi-omics database for rapeseed so far, and two case studies demonstrated its power to mine candidate genes associated with specific traits and analyze their potential regulatory mechanisms.

Key words: *Brassica napus*, multi-omics, database, candidate gene mining, functional genomics

Introduction

For comprehensive understanding of the mechanism underlying crop trait formation, it is important to interpret the molecular intricacy and variation at multiple levels such as the genome, epigenome, transcriptome, proteome, metabolome and phenome (Edwards and Batley, 2004; Li et al., 2016; Fernie and Gutierrez-Marcos, 2019; Tuggle et al., 2022). In recent years, the rapid advancement in multi-omics techniques has provided researchers with more multidimensional information to dissect complex biological systems (Ichihashi et al., 2020; Wu et al., 2021; Yang et al., 2021). Based on massive multi-omics datasets, numerous research methods have been developed to mine genetic loci and candidate genes regulating phenotypes, such as genome-wide association study (GWAS) (Yu et al., 2006), expression quantitative trait locus (eQTL) mapping(Goring et al., 2007), transcriptome-wide association study (TWAS) (Gusev et al., 2016) and summary data-based Mendelian randomization analysis (SMR) (Zhu et al., 2016). These methods have high efficiencies in mining genetic loci and candidate genes associated with certain traits and have been widely applied in crop breeding (Yu *et al.*, 2006; Wang et al., 2018; Lu et al., 2019; Liu et al., 2020; Tang et al., 2021; Zhang et al., 2021; He et al., 2022; Zhang et al., 2022a; Zhang et al., 2022b). Multi-omics techniques are becoming increasingly important in assisting crop breeding (Yang *et al.*, 2021). For more efficient utilization of multi-omics data, multi-omics databases have been developed in some important crops, such as wheat (*Triticum aestivum* L.) (Ma et al., 2021), soybean (*Glycine max*) (Grant et al., 2010), tomato (*Solanum lycopersicum*) (Kudo et al., 2017), barley (*Hordeum vulgare* L.) (Li et al., 2022), maize (*Zea mays* L.) (Gui et al., 2020), millet (*Setaria italica* L.) (Yang et al., 2020), cotton (*Gossypium hirsutum* L.) (Yang et al., 2022b) and rice (*Oryza sativa* L.) (Sakai et al., 2013).

Rapeseed is the second most important oilseed crop widely planted in the world. The traits including yield, seed oil content (SOC), oil quality, disease resistance and stress resistance largely determine its production and economic value (Friedt et al., 2018). Due to its special origin and evolutionary history, rapeseed has a polyploid genome and

therefore a more complex sequence composition and regulatory mechanism than diploid crops, which increases the difficulty in fine mapping of the candidate loci and genes (Chalhoub et al., 2014; Friedt et al., 2018). Recently, a large number of genetic loci and candidate genes associated with important traits have been efficiently identified using powerful multi-omics techniques and analysis tools (Lu *et al.*, 2019; Tang *et al.*, 2021; He *et al.*, 2022; Hu et al., 2022; Zhang *et al.*, 2022b). However, the identification is still rather time-consuming, and the regulatory mechanisms of most identified candidate loci or genes on phenotypes remain elusive. In our recent work, we have constructed and released several databases, including BnPIR (Song et al., 2021) (http://cbi.hzau.edu.cn/bnapus/), BnTIR (Liu et al., 2021a) (http://yanglab.hzau.edu.cn/BnTIR/) and BnVIR (Yang et al., 2022a) (http://yanglab.hzau.edu.cn/BnVIR/), by collecting multi-omics data including genome, transcriptome and population genetic variations and developing related omics tools. These databases have been widely applied to facilitate related research work. However, there is still a lack of platforms that integrate multi-omics data to help genetic breeding and functional genomics analysis in rapeseed.

In this study, we constructed BnIR (http://yanglab.hzau.edu.cn/BnIR/), the first *Brassica napus* multi-omics information resource database. BnIR integrates the most comprehensive multi-omics datasets involving various dimensions. In the database, multiple association analysis tools can be applied to mine the genetic loci, candidate genes and genetic variations, providing important resources, tools and references for rapeseed breeding. In addition, BnIR provides numerous common online multi-omics data analysis tools, which can support all published rapeseed genomes and offers a convenient and efficient analysis platform. We believe that BnIR will be a valuable database for future rapeseed breeding and functional genomics research.

Results

Construction and overview of BnIR

For a comprehensive understanding of rapeseed genomics, we first acquired and integrated rapeseed multi-omics data from recent research and databases. In total, datasets from six omics were obtained, including 29 genome assemblies (Supplementary Table S1), genetic variations of 2,311 accessions, transcriptome data from 2,791 libraries (Supplementary Table S2), 118 phenotypes (Supplementary Table S3), the contents of 266 metabolites and epigenome signals involving DNA methylation, histone modification, chromatin accessibility and chromatin interaction (Supplementary Table S4). Next, the related information was mined by processing and analyzing of these datasets. In addition, multiple multi-omics analysis methods were employed to mine the genetic loci, candidate genes and genetic variations, including GWAS, eQTL, TWAS, SMR and co-localization analysis. Finally, a comprehensive rapeseed multi-omics information resource database (BnIR; http://yanglab.hzau.edu.cn/BnIR/) was constructed (Figure 1).

BnIR comprises 12 portals, including Population, Genomics, Transcriptomics, Variation, Phenotype, Epigenetics, Metabolome, Multi-omics and Network, Tools, Download and Help. Abundant and convenient visual tools are provided in these portals for browsing and comparing the germplasm resource information, genome sequences, gene structures, epigenetic signals, metabolite contents and phenotypes, so as to manage germplasm resource and assist the exploring of mechanism underlying gene regulation and evolution.

New features in omics portals

Genomics. Based on our previous BnPIR database, we added Darmor (v.10), Ningyou7 and Express617 genome assemblies as well as their genome sequences and annotations, which can be downloaded from the Genome data module (Supplementary Table S1). Genome synteny and gene index have been updated, which can be browsed in the Gbrowse synteny and Gene index modules. According to the phylogenetic trees of

homologous genes, the Gene search module was developed for users to browse and compare the gene structures to determine whether the homologous genes have undergone functional differentiation at the sequence level. In addition, the gene families and transcription factors (TF) of 12 *B. napus* genome assemblies are annotated, which can be browsed in the corresponding modules of the Genomics portal.

Transcriptomics. As for the Transcriptomics portal, the previous core function modules in BnTIR, including gene expression pattern query and eFP browser, have been integrated into eFP(single gene module) and eFP(multiple gene module) of BnIR. In two eFP modules, the webpage has been redesigned to greatly improve the response speed by more than 150 times (from 9.348 s to 0.0611 s). In addition, the published RNA datasets from 537 RNA-seq libraries involving seven hormone treatments and six abiotic stress treatments have been added into the eFP modules (Supplementary Table S2). Users can browse and compare the gene expression pattern between the treatment and control groups.

In order to acquire gene expression data from more accessions, the RNA-seq data of 2,791 published tissue samples were collected, processed and summarized (Supplementary Table S2). Finally, the gene expression data of these samples were integrated into the Expression profile (meta library) module of the Transcriptomics portal, in which users can browse the expression of interested genes in all samples. As for the breeding of *B. napus*, ecotype and seed quality improvement are two key periods. In addition, heterosis is an important phenomenon and widely used for genetic improvement. To facilitate studies of the genes involved in these improvement processes, we collected the gene expression datasets from eight representative cultivars of three ecotypes, double-high (high erucic acid and high glucosinolate) and double-low (low erucic acid and low glucosinolate) cultivars (Zhongyou821 and Zhongshuang11), and eight RNA-seq datasets of accessions with heterosis. Users can browse and compare the expression levels of interested genes between different accessions in the Expression profile (meta library) module to determine whether the

150 gene is related to the breeding improvement process. In addition, we collected and
151 processed the population-level gene expression datasets in leaves and seeds at 20 and
152 40 days after flowering (DAF). Users can browse the population-level expression
153 patterns of the interested genes in the Population expression module. In summary, new
154 transcriptomic information and tools will help researchers to understand the function
155 and expression features of the interested genes from a broader perspective.

156 **Variation and phenotype.** The previous BnVIR database integrated 10,090,561
157 genetic variations and 21 phenotypes of 2,311 core *B. napus* accessions (Yang et al.,
158 2022a). On this basis, we newly collected 216 published phenotype datasets from 13
159 studies (Bus et al., 2011; Sun et al., 2016b; Sun et al., 2016a; Chen et al., 2018; Kittipol
160 et al., 2019; Wu et al., 2019; Song et al., 2020; Xuan et al., 2020; Liu et al., 2021c; Liu
161 et al., 2021b; Wang et al., 2021; Zhang *et al.*, 2021; Zhang *et al.*, 2022a) (Supplementary
162 Table S3). These datasets cover a variety of phenotypic traits, such as agronomic traits
163 under abiotic stress conditions and seed quality traits, and have been integrated into the
164 Phenotype and Variation portals. Users can browse the phenotypic values and compare
165 them between the accessions of different ecotypes in the Phenotype portal to check
166 whether the phenotype is related to ecotype improvement. In the Variation portal, users
167 can compare the phenotypic value between accessions with different alleles or
168 haplotypes to explore the effect of genetic variation on these phenotypes (Korber et al.,
169 2015; Korber et al., 2016)

170 **Epigenome.** For epigenetic data, we collected the ChIP-seq and WGBS datasets for
171 five tissues of six accessions including six histone modifications, ATAC-seq datasets
172 for seeds of four accessions and Hi-C datasets of three accessions (Supplementary Table
173 S4). After filtering and processing, a total of 5,041,596 ChIP-seq peaks and 386,313
174 ATAC-seq peaks were obtained, which were integrated into the Histone modification
175 and Chromatin accessibility modules, respectively. Based on the WGBS datasets, the
176 CG, CHG and CHH methylation levels of genes were obtained and integrated into the
177 DNA methylation module. Based on the Hi-C datasets, chromatin interaction frequency

178 and compartments were calculated and integrated into the Chromatin interaction
179 module. In addition, users can browse the tracks of all epigenetic data of the gene
180 segment of interest using the JBrowser or query these epigenetic datasets in the
181 corresponding module of the Epigenetic portal. These datasets integrated the epigenetic
182 information involving histone modification, epigenomic state, chromatin accessibility
183 and interaction, providing the first systematic epigenetic data resource in *B. napus* to
184 help identify regulatory elements in *B. napus* genome and understand their regulatory
185 mechanism.

186 **Metabolome.** In the Metabolome portal, the data about the contents of 266 metabolites
187 of two accessions from two studies were collected and integrated. Users can query the
188 related information of these metabolites, such as structure, molecular formula and
189 content in these accessions in the corresponding module, which provides a way to
190 quickly obtain the information of metabolites.

191 Integration and analysis of multi-omics data

192 Based on the collected population-level multi-omics data, we performed GWAS, eQTL
193 and TWAS to mine candidate genes and genetic variations associated with phenotypes.
194 A total of 379 loci were identified to be significantly associated with 55 phenotypes by
195 GWAS, involving 2,119 candidate genes (Supplementary Table S5). By using the
196 population-level gene expression datasets from seeds at 20 and 40 DAF of 309
197 accessions, 1,118,218 eQTLs involving 968,375 lead SNPs (eSNPs) and 33,507 genes
198 (eGenes) were identified, including 356,112 *cis*-eQTLs and 762,106 *trans*-eQTLs. In
199 total, 3,724 genes were identified to be significantly associated with 124 phenotypes by
200 TWAS (Supplementary Table S7). Next, to more precisely identify the candidate genes
201 associated with phenotypes by combining the three omics datasets, co-localization and
202 SMR analyses were performed based on the GWAS and eQTL results (Supplementary
203 Tables S8 and S9). As a result, co-localization analysis identified 130 genes
204 significantly associated with 24 phenotypic datasets; SMR identified 298 genes
205 significantly associated with 45 phenotypic datasets. By combining TWAS, co-

206 localization analysis and SMR results, a total of 3,991 genes were found to be
207 significantly associated with 131 phenotypes (Figure 2A). Known associations reported
208 in previous studies were also identified in our analysis, such as *BnaC09.MYB28* for
209 seed glucosinolate content (SGC) (Case study 1), and *BnaA05.PMT6* for SOC,
210 suggesting that the analysis results are reproducible (Supplementary Table S8). In
211 addition, some new candidate genes were found to be related to important traits, such
212 as *BnaC07.SRK2D* for SOC (Case study 2), suggesting that the analysis can be used to
213 mine new candidate genes.

214 Based on the above results, GWAS, eQTL, TWAS, COLOC, and SMR modules in
215 the Multi-omics portal were designed for convenient browsing and use of these datasets.
216 For example, users can browse information about the global GWAS signals and
217 significant variations for the phenotypes of interest in the GWAS module. Taking the
218 erucic acid content as an example, when users select 'Erucic acid' in the Trait box and
219 submit it (Figure 2B), the page will display the Manhattan plot of global GWAS results,
220 showing that the locus on chromosome A08 is the most significant locus (Figure 2C).
221 Then, the user can scroll the mouse to magnify this locus and select the region of
222 "A08:18500000–19000000" to browse for the related information of significant
223 variations (Figure 2D). Combined with the gene annotations, two non-synonymous
224 mutations in the reported candidate gene (*BnaA08.FAE1*) for erucic acid content in
225 seeds were both identified in our GWAS results (Figure 2E). In the eQTL module, users
226 can browse the genome-wide information about *cis*-eSNPs and *trans*-eSNPs regulating
227 gene expression levels. For example, the expression level of *BnaA09.ARF18* was
228 reported to be associated with the silique length and thousand-seed weight (Liu et al.,
229 2015). When users enter 'BnaA09G0559300ZS' (*BnaA09.ARF18*) and submit it
230 (Figure 2F), the page will display a list and a circus figure of 12 eQTLs regulating its
231 expression level (Figure 2G), including four *cis*-eSNPs near *BnaA09.ARF18* and eight
232 *trans*-eSNPs from four chromosomes (Figure 2H). Additionally, users can browse the

information of candidate genes associated with phenotypes identified by three methods respectively in the TWAS, SMR, and COLOC modules.

Development and application of multi-omics tools

To provide a more convenient and user-friendly platform for researchers, we developed and integrated 18 multi-omics data analysis tools in BnIR, including some common bioinformatics analysis tools, such as GO and KEGG enrichment analysis, BLAST, multi-sequence alignment (MSA), sequence extraction, variation annotation, primer design, electronic PCR and four graph visualization tools, which were all integrated into the Tools portal (Figure 3). Notably, most of analysis tools support 28 published *Brassica* genomes, and users can conduct these analyses without switching between different platforms. For population-level multi-omics data analysis, OnlineGWAS module can help users to perform GWAS by uploading phenotypic datasets. And we newly developed COLOC and SMR online analysis and visualization tools based on the rapeseed eQTL results of our database, which allow users to identify candidate genes and causal variants by uploading GWAS results. In addition, to facilitate the identification of germplasm resources, the SNPmatch tool based on the genetic variation dataset of 2,311 accessions was integrated into the Tool portal (Pisupati et al., 2017). In the SNPmatch module, the user can identify the accession with the highest similarity to their accession by uploading the genotype of the sample.

In summary, BnIR provides abundant and comprehensive multi-omics data resources and convenient analysis tools. As a high-efficiency data analysis platform, BnIR allows direct utilization of these data and tools to mine genetic loci, genes and variations associated with specific traits. Furthermore, BnIR can also facilitate understanding of the mechanisms for gene expression regulation and phenotypic formation in the *B. napus* genome from different omics dimensions.

Case study 1: Mining of genes associated with seed glucosinolate content.

SGC is an important trait related to the oil quality of rapeseed (Gupta and Pratap, 2007;

261 Wang et al., 2018; Lu et al., 2019). In order to mine the genes related to SGC, GWAS
262 was first performed. By using the GWAS module of the Multi-omics portal, the
263 'Glucosinolate content' phenotype was selected for browsing significant GWAS signals
264 (Figure 4A). As a result, a total of 20 genetic loci distributed in 10 chromosomes were
265 identified to be associated with SGC (Figure 4B and Supplementary Table S5). Among
266 them, *qGLS.C09.8* containing *BnaC09.MYB28a* and *BnaC09.MYB28b* was the most
267 significant locus with the strongest effect (Figure 4C). *BnaC09.MYB28a* and
268 *BnaC09.MYB28b* are members of the large family of R2R3-MYB transcription factors
269 and have been identified as regulators of glucosinolate biosynthetic genes in *B. napus*
270 (Harper et al., 2012; Wang et al., 2018). Notably, the most significant variations were
271 distributed around *BnaC09.MYB28a* and *BnaC09.MYB28b* and showed strong linkage
272 disequilibrium (LD) (Figure 4D). To further determine whether these two
273 *BnaC09.MYB28s* are related to SGC, TWAS and co-localization analysis were
274 performed. By using the TWAS module to browse the results, *BnaC09.MYB28a* and
275 *BnaC09.MYB28b* were both found to be significantly associated with SGC
276 (Supplementary Table S7), suggesting that their expression levels can potentially
277 influence SGC. Then, the COLOC module was used to further test whether the GWAS
278 locus and the *cis*-eQTLs of *BnaC09.MYB28a* and *BnaC09.MYB28b* are co-localized
279 (Figure 4E). The two *BnaC09.MYB28s* and the 'Glucosinolate content' phenotype were
280 selected to query their co-localization analysis results (Figure 4E). As a result, they
281 shared the same causal variant (PPH_4 = 0.99), suggesting that *BnaC09.MYB28a* and
282 *BnaC09.MYB28b* are candidate genes associated with SGC (Figure 4F and G). In
283 addition, frameshift mutation (GCTA/-) may be the causal variation, which has been
284 analyzed in our previous research (Wang *et al.*, 2018; Yang *et al.*, 2022a) (Figure 4F
285 and G).

286 Case study 2: Identification of new genes associated with seed oil 287 content

288 SOC is one of the most important traits of rapeseed (Wang *et al.*, 2018; Tang *et al.*,

289 2021). Here, the published SOC data of 286 *B. napus* accessions were used to validate
290 the power of BnIR in identifying new candidate genes associated with traits (Wang *et*
291 *al.*, 2021). First, five significant loci were identified using GWAS, among which
292 *qOC.C07.1* was the most significant locus. Then, the GWAS module in BnIR was used
293 to browse the GWAS results in this locus (Supplementary Figure 1A). Significant
294 variations were mainly distributed near *BnaC07.SRK2D* (BnaC07G0388200ZS) with
295 strong LD (Supplementary Figure 1B). *BnaC07.SRK2D* encodes a member of abscisic
296 acid (ABA)-activated SNF1-related protein kinases (*SnRK2*), which play important
297 roles in various seed developmental processes such as de-greening, accumulation of
298 seed storage products, seed maturation, desiccation tolerance and germination
299 (Nakashima and Yamaguchi-Shinozaki, 2013; Lin et al., 2021; Ali et al., 2022; Kozaki
300 and Aoyanagi, 2022). Next, we attempted to check whether the expression of
301 *BnaC07.SRK2D* is related to SOC through co-localization analysis. When users enter
302 the COLOC module of the Multi-omics portal and then select the eQTL of
303 *BnaC07.SRK2D* and the QTL of SOC in GWAS (Figure 5A), the co-localization
304 analysis results would be showed on the page (Figure 5B-D), which indicated that they
305 shared the same causal variation, suggesting that *BnaC07.SRK2D* is a candidate gene
306 for SOC.
307 Then, we used the Variation portal to further explore how genetic variation in this
308 locus affects gene expression and ultimately influences the phenotype of the population.
309 When entering 'BnaC07G0388200ZS' in gene box of the Single-locus module of the
310 Variation portal and choosing the 1 kb of flanking region (Figure 5E), we obtained 13
311 variations in this gene region, including ten variations in the upstream or downstream
312 of the gene and three in the genic region (Figure 5F). Next, we performed a haplotype
313 analysis to examine their effects on the gene expression and phenotype. When selecting
314 these variations in the Multi-locus module (Figure 5G), we obtained two haplotypes
315 with a frequency higher than 0.05 (Figure 5H and I). We found that the accessions with
316 Hap2 (the same as Zhongshuang 11, a representative accession with high SOC; mean

317 SOC, 48.51%) had significantly higher gene expression and SOC than those with Hap1
318 (mean SOC, 43.22%) (Figure 5H and I). These results indicated that these significant
319 variations contribute to the divergence in the expression of *BnaC07.SRK2D* and
320 phenotype. In other words, the accessions with Hap2 had significantly higher
321 expression levels of *BnaC07.SRK2D*, which eventually contribute to higher SOC. Such
322 findings will provide a valuable reference for increasing SOC in future breeding.
323

324 **Discussion**

325 In this study, we first collected and processed rapeseed multi-omics data from recent
326 research and databases, and then constructed BnIR, the first rapeseed multi-omics
327 database. BnIR provides comprehensive multi-omics data resources, including genome
328 sequences, annotations and expression levels of genes, epigenetic signals, metabolite
329 contents, traits and association signals. In addition, multiple online analysis and
330 visualization tools were developed and integrated to help researchers to mine genetic
331 loci/genes and understand the regulatory mechanisms of gene expression and
332 phenotypic formation. Two case studies including mining of candidate genes associated
333 with SGC and SOC fully exhibited the power of BnIR in assisting genetic breeding.
334 Compared with the published rapeseed databases, BnIR has the following
335 characteristics. 1) It integrates and optimizes the data sources and functions of BnPIR,
336 BnTIR and BnVIR, and significantly improves the scale of the data source and response
337 speed of the webpage (Figure 6A). 2) To the best of our knowledge, BnIR comprises
338 the most comprehensive multi-omics datasets, including 13 published genome
339 assemblies, genetic variations of 2,311 accessions, transcriptome data from 2,791
340 libraries, 118 phenotypes, contents of 266 metabolites, and multiple epigenome data
341 involving histone modification, chromatin accessibility and chromatin interaction
342 (Figure 6B). 3) GWAS, eQTL, TWAS, SMR and co-localization analysis are applied to
343 mine the genetic loci, candidate genes and genetic variations, providing important
344 resources, tools and references for rapeseed breeding (Figure 6B). 4) BnIR provides

numerous common online multi-omics data analysis tools, which support all published rapeseed genomes and provide a convenient and efficient analysis platform.

In summary, we provide a valuable database for future rapeseed breeding and functional genomics research. In the future, with the release of more multi-omics datasets, we will update the database annually. In addition, more newly developed high-efficiency multi-omics methods will be applied to mine more candidate loci and genes associated with traits. These efforts will make BnIR a more useful platform in rapeseed research.

354 # Materials and Methods

355 ## Data sources

356 To obtain comprehensive rapeseed multi-omics datasets, we mined and integrated the
357 data from genomics, transcriptomics, genetic variations, phenotypic data, epigenetics
358 and metabolomics (Figure 1; Supplementary Tables S1, S2, S3, S4). In total, 29
359 published *Brassica* genome assemblies (including 14 *B. napus* genome assemblies) and
360 2,290,519 genes in them were collected (Supplementary Table S1). As for the
361 Transcriptome portal, 2,791 RNA-seq libraries of 272 individuals for 23 tissues were
362 collected from published studies and databases (including 91 libraries from BnTIR)
363 (Liu *et al.*, 2021a), which are listed in Supplementary Table S2. As for the phenotypic
364 data, the data of 118 phenotypes of 2,512 accessions were collected from 13 published
365 studies (Figure 2; Supplementary Table S3). The epigenetics data are summarized in
366 Supplementary Table S4. Metabolome datasets were retrieved from two previous
367 studies (Geng et al., 2017; Clement et al., 2018). Genetic variation datasets of 2,311
368 accessions from BnVIR were also integrated into BnIR (Yang *et al.*, 2022a).

369 ## Reanalysis of omics datasets

370 For the omics datasets from different studies, considering the differences in data
371 processing and analysis processes, unified pipelines and parameters were used for
372 reanalysis of datasets during integration.

373 **Genome annotation.** For three newly collected *B. napus* genome assemblies, the
374 repeat sequences were predicted as previously described and then integrated into the
375 GBrowse of Genome synteny module (McKay et al., 2010; Song *et al.*, 2020). The gene
376 families, transcription factors, GO terms and KEGG pathways of all genome assemblies
377 were predicted according to their homology to the *A. thaliana* genome and the
378 annotations of *A. thaliana* downloaded from TAIR (https://www.arabidopsis.org/).

379 **Comparative genome analysis.** Genome sequences were compared between ZS11
380 reference genome and other 11 *B. napus* and two diploid (Z1 and HDEM) genome
381 assemblies using the NUCmer program (v.4.0.0beta2) with parameters "nucmer --mum

382 –noextend" in MUMmer4 (Marcais et al., 2018). After filtering of the one-to-one
383 alignments with a minimum alignment length of 50 bp using the show-diff program
384 from MUMmer4, the remaining alignment blocks were used for genome browser
385 visualization. For genome browser visualization, the Dotplot module in JBrowse2 and
386 Genome synteny module in GBrowser were embedded in BnIR (McKay *et al.*, 2010;
387 Hofmeister and Schmitz, 2018).

388 A total of 1,185,955 genes from 12 *B. napus* genome assemblies were used to
389 construct the gene clusters. First, protein sequences of every pair from 12 genome
390 assemblies were aligned using DIAMOND (v.0.9.14.115,
391 http://github.com/bbuchfink/diamond). Then, gene synteny was detected by McScan
392 (python version). The genes with synteny were grouped into one cluster. Finally, these
393 genes were grouped into 231,106 gene clusters.

394 **Transcriptome analysis.** After clipping adaptor sequences and removing low-quality
395 reads by fastp (v. 0.23.0), the clean RNA-seq data from accessions were mapped to the
396 ZS11 reference genome using Hisat2 (v.2.1.2) with default parameters (Kim et al.,
397 2015). Gene expression levels were normalized using the number of transcripts per
398 kilobase million reads (TPM) by the StringTie software (v.1.3.5) with default
399 settings(Pertea et al., 2015). The co-expression network was obtained by calculating
400 the Pearson correlation coefficient of pairwise gene expression levels, and the gene
401 modules including the gene pairs with a Pearson correlation coefficient higher than 0.8
402 were retained as a co-expression network.

403 **Epigenome analysis.** The methods used to remove adaptor sequences and filter low-
404 quality reads were the same as those in RNA-seq data analysis. As for ChIP-seq and
405 ATAC-seq, the clean data from accessions were mapped to the ZS11 reference genome
406 using bowtie2 (v.2.3.2) with default parameters (Langmead and Salzberg, 2012). PCR
407 duplicate reads were removed using Picard (v.2.19,
408 http://broadinstitute.github.io/picard/). Peaks were called using the callpeak module of
409 MACS2 software (v.2.1.2) with the parameters " --broad -f BAM -g 1000000000 -B -p

410 0.00001 --nomodel --extsize 147 " (Feng et al., 2012).

411 As for Hi-C, the clean reads of each accession were mapped to the ZS11 reference
412 genome using BWA-MEM with default parameters (Li and Durbin, 2009; Song *et al.*,
413 2020). Then, the Hi-C interaction matrix was created using the Juicer pipeline (Durand
414 et al., 2016). The KR-normalized matrix was extracted from Hi-C format files at the
415 resolutions of 10 kb, 50 kb and 100 kb using the Juicer_tools (v.1.7.6) for JBrowser
416 (Rao et al., 2014; Buels et al., 2016), and then compartments were called using
417 Juicer_tools at the resolution of 100 kb.

418 As for the BS-seq data, clean data of each accession were mapped to the ZS11
419 reference genome using Bismark (v.0.13.0) with the parameter settings "-N 1, -L 30"
420 (Krueger and Andrews, 2011). BigWig files of all epigenome data analysis can be
421 visited by JBrowser in the Tools portal (Buels *et al.*, 2016).

422 **GWAS.** As for the phenotypic datasets from different studies, GWAS was performed
423 using the common pipeline. First, the SNPs and InDels with a minor allele frequency
424 (MAF) lower than 0.05 were filtered. Then, GWAS was performed using GEMMA
425 (v.0.98.1) (Zhou and Stephens, 2012). The population structure was controlled by
426 including the first three principal components as covariates, as well as an IBS kinship
427 matrix derived from all variants (SNPs and InDels) calculated by GEMMA. The cutoff
428 for determining significant associations was set as $-\log_{10}(1/n)$, where n represents the
429 total number of variations. Finally, genetic loci and lead variation were identified with
430 the following steps. 1) Two significant variations were regarded as the same locus if the
431 distance between them was less than 0.5 Mb and; 2) As for a genetic locus, the most
432 significant variation associated with the phenotype was identified as the lead SNP.

433 **eQTL mapping.** Gene expression values were taken as the values of the phenotype for
434 eQTL mapping. Only those genes expressed in more than 95% of the accessions were
435 defined as expressed genes for eQTL mapping. Variations with MAF > 5% were used
436 to perform GWAS for each gene by using GEMMA to detect the associations for
437 variations and genes (Zhou and Stephens, 2012). The cutoff for determining significant

438 associations was set as $-\log_{10}(1/n)$, where n represents the total number of variations.
439 Based on the distance between eQTLs and targeted-genes, we subdivided all eQTLs
440 into cis-eQTLs if the variation was found within 1 Mb of the transcription start site or
441 transcription end site of the target gene, otherwise as trans-eQTLs. In BnIR, the
442 regulatory pairs of eQTLs and eGenes are visualized using BioCircos.js (Cui et al.,
443 2016).
444 **TWAS.** TWAS was used to integrate GWAS and gene expression datasets to identify
445 gene-trait associations (Gusev *et al.*, 2016). TWAS was conducted by the EMMAX
446 module using the gene expression data of seeds at 20 DAF and 40 DAF with the data
447 of the phenotypes from the same accessions. Models were considered as
448 'transcriptome-wide significant' if they passed the Bonferroni correction for all genes.
449 **SMR analysis.** SMR analysis integrated the summary-level data from GWAS with
450 eQTL data to identify genes associated with a complex trait considering their pleiotropy.
451 The *cis*-eQTL signals of expressed genes and GWAS signals of the phenotype were
452 used to perform SMR analysis and HEIDI test by SMR software (v.1.03) (Gusev *et al.*,
453 2016). Then, the gene was defined as a candidate gene of the phenotype when the -
454 $\log_{10}$(P-value) of SMR was lower than 1/n (n is the number of all expressed protein-
455 coding genes) and P-value of HEIDI test was higher than 1.57×10^{-3}.
456 **Co-localization analysis.** GWAS loci associated with phenotypes and candidate genes
457 in these loci were used for co-localization analysis performed using the "COLOC" R
458 package with default parameters (Hormozdiari et al., 2016). The variants in *cis*-eQTLs
459 of genes and QTLs of phenotypes were defined as co-localized when the posterior
460 probability of a co-localized signal (PPH_4) value was higher than 0.5 and there was at
461 least one shared significant variation.
462 **GO and KEGG enrichment analysis.** The GO and KEGG enrichment analysis was
463 as follows: Firstly, we used blastp to establish homologous gene pairs of each rapeseed
464 genome and Arabidopsis genome(Camacho et al., 2009; Boratyn et al., 2013), and then
465 assigned the genes in the rapeseed genome according to the GO and KEGG annotation

results of the Arabidopsis genome. Next, GO and KEGG libraries were established for each rapeseed genome using the 'clusterProfiler' R package(Yu et al., 2012). Finally, based on the GO and KEGG libraries, the 'clusterProfiler' R package was used for GO and KEGG enrichment analysis according to the gene list input by users.

Implementation

BnIR (http://yanglab.hzau.edu.cn/BnIR) was constructed based on the ThinkPHP (v.5.0.24) framework with jQuery (v.3.6.0) as the JavaScript library, and runs on the Apache 2 web server (v.2.4.53) with MySQL (v.8.0.29) as its database engine. The database is available online without registration and optimized for Chrome (recommended), Opera, Firefox, Windows Edge and macOS Safari.

DATA AVAILABILITY

Sources of all datasets are described in supplemental materials and methods. All datasets are made available at http://yanglab.hzau.edu.cn/BnIR/download.

FUNDING

This research was supported by the National Natural Science Foundation of China (32070559), the National Key Research and Development Plan of China (2021YFF1000100), China Postdoctoral Science Foundation (2022M710875), Hubei Hongshan Laboratory (2021HSZD004) and Developing Bioinformatics Platform in Hainan Yazhou Bay Seed Lab (No. JBGS-B21HJ0001).

Conflict of interest statement. None declared.

Author contributions

Q.-Y.Y. designed the project. Q.-Y.Y. and Z.Y. managed and coordinated the project. Z.Y., S.W., Y.M.H., C.L., Y.J., Y.L. and Y.H. collected datasets and performed the bioinformatics analysis. Q.-Y.Y., Z.Y. and D.L designed the database; S.W., Y.M.H., L.W. and D.L. constructed the database. Q.-Y.Y., Z.Y., S.W. and Y.M.H wrote the manuscript. Q.-Y.Y., Y.Z., L.G. and C.D. directed the project.

ACKNOWLEDGEMENTS

We thank Prof. Kede Liu from Huazhong Agricultural University of China, Prof. Kun Lu from Southwest University of China, Dr. Wujian from Yangzhou University of China, and other researchers for many very good and constructive feedback and suggestions in improving BnIR. We thank bioinformatics computing platform of the National Key Laboratory of Crop Genetic Improvement, Huazhong Agricultural University, managed by Hao Liu.

Reference

Ali, F., Qanmber, G., Li, F., and Wang, Z. (2022). Updated role of ABA in seed maturation, dormancy, and germination. J. Adv. Res. **35**:199-214.

Boratyn, G.M., Camacho, C., Cooper, P.S., Coulouris, G., Fong, A., Ma, N., Madden, T.L., Matten, W.T., McGinnis, S.D., Merezhuk, Y., et al. (2013). BLAST: a more efficient report with usability improvements. Nucleic Acids Res. **41**:W29-33.

Buels, R., Yao, E., Diesh, C.M., Hayes, R.D., Munoz-Torres, M., Helt, G., Goodstein, D.M., Elsik, C.G., Lewis, S.E., Stein, L., et al. (2016). JBrowse: a dynamic web platform for genome visualization and analysis. Genome Biol. **17**:66.

Bus, A., Korber, N., Snowdon, R.J., and Stich, B. (2011). Patterns of molecular variation in a species-wide germplasm set of *Brassica napus*. TAG. Theoretical and applied genetics. Theoretische und angewandte Genetik **123**:1413-1423.

Camacho, C., Coulouris, G., Avagyan, V., Ma, N., Papadopoulos, J., Bealer, K., and Madden, T.L. (2009). BLAST+: architecture and applications. BMC Bioinformatics **10**:421.

Chalhoub, B., Denoeud, F., Liu, S., Parkin, I.A., Tang, H., Wang, X., Chiquet, J., Belcram, H., Tong, C., Samans, B., et al. (2014). Plant genetics. Early allopolyploid evolution in the post-Neolithic *Brassica napus* oilseed genome. Science **345**:950-953.

Chen, L., Wan, H., Qian, J., Guo, J., Sun, C., Wen, J., Yi, B., Ma, C., Tu, J., Song, L., et al. (2018). Genome-wide association study of cadmium accumulation at the seedling stage in rapeseed (*Brassica napus* L.). Front. Plant Sci. **9**:375.

Clement, G., Moison, M., Soulay, F., Reisdorf-Cren, M., and Masclaux-Daubresse, C. (2018). Metabolomics of laminae and midvein during leaf senescence and source-sink metabolite management in *Brassica napus* L. leaves. J. Exp. Bot. **69**:891-903.

Cui, Y., Chen, X., Luo, H., Fan, Z., Luo, J., He, S., Yue, H., Zhang, P., and Chen, R. (2016). BioCircos.js: an interactive Circos JavaScript library for biological data visualization on web applications. Bioinformatics **32**:1740-1742.

Durand, N.C., Shamim, M.S., Machol, I., Rao, S.S., Huntley, M.H., Lander, E.S., and Aiden, E.L. (2016). Juicer provides a one-click system for analyzing loop-resolution Hi-C experiments. Cell Syst. **3**:95-98.

Edwards, D., and Batley, J. (2004). Plant bioinformatics: from genome to phenome. Trends Biotechnol. **22**:232-237.

Feng, J., Liu, T., Qin, B., Zhang, Y., and Liu, X.S. (2012). Identifying ChIP-seq enrichment using MACS. Nat. Protoc. **7**:1728-1740.

Fernie, A.R., and Gutierrez-Marcos, J. (2019). From genome to phenome: genome-wide association studies and other approaches that bridge the genotype to phenotype gap. Plant J. **97**:5-7.

Friedt, W., Tu, J., and Fu, T. (2018). Academic and economic importance of *Brassica*

napus rapeseed. In The Brassica napus Genome, S. Liu and R. Snowdon and B. Chalhoub, eds. (Springer International Publishing: Cham), pp. 1-20.

Geng, S., Yu, B., Zhu, N., Dufresne, C., and Chen, S. (2017). Metabolomics and proteomics of *Brassica napus* guard cells in response to Low CO_2. Front. Mol. Biosci. **4**:51.

Goring, H.H., Curran, J.E., Johnson, M.P., Dyer, T.D., Charlesworth, J., Cole, S.A., Jowett, J.B., Abraham, L.J., Rainwater, D.L., Comuzzie, A.G., et al. (2007). Discovery of expression QTLs using large-scale transcriptional profiling in human lymphocytes. Nat. Genet. **39**:1208-1216.

Grant, D., Nelson, R.T., Cannon, S.B., and Shoemaker, R.C. (2010). SoyBase, the USDA-ARS soybean genetics and genomics database. Nucleic Acids Res. **38**:D843-846.

Gui, S., Yang, L., Li, J., Luo, J., Xu, X., Yuan, J., Chen, L., Li, W., Yang, X., Wu, S., et al. (2020). ZEAMAP, a Comprehensive Database Adapted to the Maize Multi-Omics Era. iScience **23**:101241.

Gupta, S.K., and Pratap, A. (2007). History, Origin, and Evolution. In Advances in Botanical Research, (Academic Press: pp. 1-20.

Gusev, A., Ko, A., Shi, H., Bhatia, G., Chung, W., Penninx, B.W.J.H., Jansen, R., de Geus, E.J.C., Boomsma, D.I., Wright, F.A., et al. (2016). Integrative approaches for large-scale transcriptome-wide association studies. Nat. Genet. **48**:245-252.

Harper, A.L., Trick, M., Higgins, J., Fraser, F., Clissold, L., Wells, R., Hattori, C., Werner, P., and Bancroft, I. (2012). Associative transcriptomics of traits in the polyploid crop species *Brassica napus*. Nat. Biotechnol. **30**:798-802.

He, Y., Yang, Z., Tang, M., Yang, Q.Y., Zhang, Y., and Liu, S. (2022). Enhancing canola breeding by editing a glucosinolate transporter gene lacking natural variation. Plant Physiol. **188**:1848-1851.

Hofmeister, B.T., and Schmitz, R.J. (2018). Enhanced JBrowse plugins for epigenomics data visualization. BMC Bioinformatics **19**:159.

Hormozdiari, F., van de Bunt, M., Segre, A.V., Li, X., Joo, J.W.J., Bilow, M., Sul, J.H., Sankararaman, S., Pasaniuc, B., and Eskin, E. (2016). Colocalization of GWAS and eQTL signals detects target genes. Am. J. Hum. Genet. **99**:1245-1260.

Hu, J., Chen, B., Zhao, J., Zhang, F., Xie, T., Xu, K., Gao, G., Yan, G., Li, H., Li, L., et al. (2022). Genomic selection and genetic architecture of agronomic traits during modern rapeseed breeding. Nat. Genet. **54**:694-704.

Ichihashi, Y., Date, Y., Shino, A., Shimizu, T., Shibata, A., Kumaishi, K., Funahashi, F., Wakayama, K., Yamazaki, K., Umezawa, A., et al. (2020). Multi-omics analysis on an agroecosystem reveals the significant role of organic nitrogen to increase agricultural crop yield. Proc. Natl. Acad. Sci. U. S. A. **117**:14552-14560.

Kim, D., Langmead, B., and Salzberg, S.L. (2015). HISAT: a fast spliced aligner with low memory requirements. Nat. Methods **12**:357-360.

Kittipol, V., He, Z., Wang, L., Doheny-Adams, T., Langer, S., and Bancroft, I.

585 (2019). Data in support of genetic architecture of glucosinolate variations in
586 *Brassica napus*. Data Brief **25**:104402.
587 **Korber, N., Bus, A., Li, J., Parkin, I.A., Wittkop, B., Snowdon, R.J., and Stich, B.**
588 (2016). Agronomic and deed quality traits dissected by genome-wide association
589 mapping in *Brassica napus*. Front. Plant Sci. **7**:386.
590 **Korber, N., Bus, A., Li, J., Higgins, J., Bancroft, I., Higgins, E.E., Parkin, I.A.,**
591 **Salazar-Colqui, B., Snowdon, R.J., and Stich, B.** (2015). Seedling development
592 traits in *Brassica napus* examined by gene expression analysis and association
593 mapping. BMC Plant Biol. **15**:136.
594 **Kozaki, A., and Aoyanagi, T.** (2022). Molecular aspects of seed development
595 controlled by gibberellins and abscisic acids. Int. J. Mol. Sci. **23**:1876.
596 **Krueger, F., and Andrews, S.R.** (2011). Bismark: a flexible aligner and methylation
597 caller for Bisulfite-Seq applications. Bioinformatics **27**:1571-1572.
598 **Kudo, T., Kobayashi, M., Terashima, S., Katayama, M., Ozaki, S., Kanno, M.,**
599 **Saito, M., Yokoyama, K., Ohyanagi, H., Aoki, K., et al.** (2017). TOMATOMICS:
600 A Web Database for Integrated Omics Information in Tomato. Plant & cell
601 physiology **58**:e8.
602 **Langmead, B., and Salzberg, S.L.** (2012). Fast gapped-read alignment with Bowtie 2.
603 Nat. Methods **9**:357-359.
604 **Li, D., Huang, Z., Song, S., Xin, Y., Mao, D., Lv, Q., Zhou, M., Tian, D., Tang, M.,**
605 **Wu, Q., et al.** (2016). Integrated analysis of phenome, genome, and transcriptome
606 of hybrid rice uncovered multiple heterosis-related loci for yield increase. Proc.
607 Natl. Acad. Sci. U. S. A. **113**:E6026-E6035.
608 **Li, H., and Durbin, R.** (2009). Fast and accurate short read alignment with Burrows-
609 Wheeler transform. Bioinformatics **25**:1754-1760.
610 **Li, T., Bian, J., Tang, M., Shangguan, H., Zeng, Y., Luo, R., Sun, H., Ke, Q., Nie,**
611 **X., Li, Y., et al.** (2022). BGFD: an integrated multi-omics database of barley gene
612 families. BMC Plant Biol. **22**:454.
613 **Lin, Z., Li, Y., Wang, Y., Liu, X., Ma, L., Zhang, Z., Mu, C., Zhang, Y., Peng, L.,**
614 **Xie, S., et al.** (2021). Initiation and amplification of SnRK2 activation in abscisic
615 acid signaling. Nat. Commun. **12**:2456.
616 **Liu, D., Yu, L., Wei, L., Yu, P., Wang, J., Zhao, H., Zhang, Y., Zhang, S., Yang, Z.,**
617 **Chen, G., et al.** (2021a). BnTIR: an online transcriptome platform for exploring
618 RNA-seq libraries for oil crop Brassica napus. Plant Biotechnol. J. **19**:1895-1897.
619 **Liu, H., Wang, J., Zhang, B., Yang, X., Hammond, J.P., Ding, G., Wang, S., Cai,**
620 **H., Wang, C., Xu, F., et al.** (2021b). Genome-wide association study dissects the
621 genetic control of plant height and branch number in response to low-phosphorus
622 stress in *Brassica napus*. Ann. Bot. **128**:919-930.
623 **Liu, H., Li, X., Zhang, Q., Yuan, P., Liu, L., King, G.J., Ding, G., Wang, S., Cai, H.,**
624 **Wang, C., et al.** (2021c). Integrating a genome-wide association study with
625 transcriptomic data to predict candidate genes and favourable haplotypes
626 influencing *Brassica napus* seed phytate. DNA Res. **28**:dsab011.

627 **Liu, J., Hua, W., Hu, Z., Yang, H., Zhang, L., Li, R., Deng, L., Sun, X., Wang, X.,**
628 **and Wang, H.** (2015). Natural variation in *ARF18* gene simultaneously affects
629 seed weight and silique length in polyploid rapeseed. Proc. Natl. Acad. Sci. U. S.
630 A. **112**:E5123-5132.
631 **Liu, S., Huang, H., Yi, X., Zhang, Y., Yang, Q., Zhang, C., Fan, C., and Zhou, Y.**
632 (2020). Dissection of genetic architecture for glucosinolate accumulations in
633 leaves and seeds of *Brassica napus* by genome-wide association study. Plant
634 Biotechnol. J. **18**:1472-1484.
635 **Lu, K., Wei, L., Li, X., Wang, Y., Wu, J., Liu, M., Zhang, C., Chen, Z., Xiao, Z.,**
636 **Jian, H., et al.** (2019). Whole-genome resequencing reveals *Brassica napus* origin
637 and genetic loci involved in its improvement. Nat. Commun. **10**:1154.
638 **Ma, S., Wang, M., Wu, J., Guo, W., Chen, Y., Li, G., Wang, Y., Shi, W., Xia, G., Fu,**
639 **D., et al.** (2021). WheatOmics: A platform combining multiple omics data to
640 accelerate functional genomics studies in wheat. Mol. Plant **14**:1965-1968.
641 **Marcais, G., Delcher, A.L., Phillippy, A.M., Coston, R., Salzberg, S.L., and Zimin,**
642 **A.** (2018). MUMmer4: A fast and versatile genome alignment system. PLoS
643 Comput. Biol. **14**:e1005944.
644 **McKay, S.J., Vergara, I.A., and Stajich, J.E.** (2010). Using the generic synteny
645 browser (GBrowse_syn). Curr. Protoc. Bioinformatics **Chapter 9**:Unit-9.12.
646 **Nakashima, K., and Yamaguchi-Shinozaki, K.** (2013). ABA signaling in stress-
647 response and seed development. Plant Cell Rep. **32**:959-970.
648 **Pertea, M., Pertea, G.M., Antonescu, C.M., Chang, T.C., Mendell, J.T., and**
649 **Salzberg, S.L.** (2015). StringTie enables improved reconstruction of a
650 transcriptome from RNA-seq reads. Nat. Biotechnol. **33**:290-295.
651 **Pisupati, R., Reichardt, I., Seren, U., Korte, P., Nizhynska, V., Kerdaffrec, E.,**
652 **Uzunova, K., Rabanal, F.A., Filiault, D.L., and Nordborg, M.** (2017).
653 Verification of Arabidopsis stock collections using SNPmatch, a tool for
654 genotyping high-plexed samples. Sci. Data **4**:170184.
655 **Rao, S.S., Huntley, M.H., Durand, N.C., Stamenova, E.K., Bochkov, I.D., Robinson,**
656 **J.T., Sanborn, A.L., Machol, I., Omer, A.D., Lander, E.S., et al.** (2014). A 3D
657 map of the human genome at kilobase resolution reveals principles of chromatin
658 looping. Cell **159**:1665-1680.
659 **Sakai, H., Lee, S.S., Tanaka, T., Numa, H., Kim, J., Kawahara, Y., Wakimoto, H.,**
660 **Yang, C.C., Iwamoto, M., Abe, T., et al.** (2013). Rice Annotation Project
661 Database (RAP-DB): an integrative and interactive database for rice genomics.
662 Plant & cell physiology **54**:e6.
663 **Song, J.M., Liu, D.X., Xie, W.Z., Yang, Z., Guo, L., Liu, K., Yang, Q.Y., and Chen,**
664 **L.L.** (2021). BnPIR: *Brassica napus* pan-genome information resource for 1689
665 accessions. Plant Biotechnol. J. **19**:412-414.
666 **Song, J.M., Guan, Z., Hu, J., Guo, C., Yang, Z., Wang, S., Liu, D., Wang, B., Lu,**
667 **S., Zhou, R., et al.** (2020). Eight high-quality genomes reveal pan-genome
668 architecture and ecotype differentiation of *Brassica napus*. Nat. Plants **6**:34-45.

669 **Sun, C., Wang, B., Yan, L., Hu, K., Liu, S., Zhou, Y., Guan, C., Zhang, Z., Li, J.,**
670 **Zhang, J., et al.** (2016a). Genome-wide association study provides insight into
671 the genetic control of plant height in rapeseed (*Brassica napus* L.). Front. Plant
672 Sci. **7**:1102.
673 **Sun, C., Wang, B., Wang, X., Hu, K., Li, K., Li, Z., Li, S., Yan, L., Guan, C., Zhang,**
674 **J., et al.** (2016b). Genome-wide association study dissecting the genetic
675 architecture underlying the branch angle trait in rapeseed (*Brassica napus* L.). Sci.
676 Rep. **6**:33673.
677 **Tang, S., Zhao, H., Lu, S., Yu, L., Zhang, G., Zhang, Y., Yang, Q.Y., Zhou, Y., Wang,**
678 **X., Ma, W., et al.** (2021). Genome- and transcriptome-wide association studies
679 provide insights into the genetic basis of natural variation of seed oil content in
680 Brassica napus. Mol. Plant **14**:470-487.
681 **Tuggle, C.K., Clarke, J., Dekkers, J.C.M., Ertl, D., Lawrence-Dill, C.J., Lyons, E.,**
682 **Murdoch, B.M., Scott, N.M., and Schnable, P.S.** (2022). The Agricultural
683 Genome to Phenome Initiative (AG2PI): creating a shared vision across crop and
684 livestock research communities. Genome Biol. **23**:3.
685 **Wang, B., Wu, Z., Li, Z., Zhang, Q., Hu, J., Xiao, Y., Cai, D., Wu, J., King, G.J.,**
686 **Li, H., et al.** (2018). Dissection of the genetic architecture of three seed-quality
687 traits and consequences for breeding in *Brassica napus*. Plant Biotechnol. J.
688 **16**:1336-1348.
689 **Wang, H., Wang, Q., Pak, H., Yan, T., Chen, M., Chen, X., Wu, D., and Jiang, L.**
690 (2021). Genome-wide association study reveals a patatin-like lipase relating to the
691 reduction of seed oil content in *Brassica napus*. BMC Plant Biol. **21**:6.
692 **Wu, D., Liang, Z., Yan, T., Xu, Y., Xuan, L., Tang, J., Zhou, G., Lohwasser, U., Hua,**
693 **S., Wang, H., et al.** (2019). Whole-genome resequencing of a worldwide
694 collection of rapeseed accessions reveals the genetic basis of ecotype divergence.
695 Mol. Plant **12**:30-43.
696 **Wu, L., Han, L., Li, Q., Wang, G., Zhang, H., and Li, L.** (2021). Using interactome
697 big data to crack genetic mysteries and enhance future crop breeding. Mol. Plant
698 **14**:77-94.
699 **Xuan, L., Yan, T., Lu, L., Zhao, X., Wu, D., Hua, S., and Jiang, L.** (2020). Genome-
700 wide association study reveals new genes involved in leaf trichome formation in
701 polyploid oilseed rape (*Brassica napus* L.). Plant Cell Environ. **43**:675-691.
702 **Yang, Y., Saand, M.A., Huang, L., Abdelaal, W.B., Zhang, J., Wu, Y., Li, J., Sirohi,**
703 **M.H., and Wang, F.** (2021). Applications of multi-omics technologies for crop
704 improvement. Front. Plant Sci. **12**:563953.
705 **Yang, Z., Liang, C., Wei, L., Wang, S., Yin, F., Liu, D., Guo, L., Zhou, Y., and Yang,**
706 **Q.Y.** (2022a). BnVIR: bridging the genotype-phenotype gap to accelerate mining
707 of candidate variations underlying agronomic traits in Brassica napus. Mol. Plant
708 **15**:779-782.
709 **Yang, Z., Zhang, H., Li, X., Shen, H., Gao, J., Hou, S., Zhang, B., Mayes, S.,**
710 **Bennett, M., Ma, J., et al.** (2020). A mini foxtail millet with an Arabidopsis-like

711 life cycle as a C4 model system. Nat. Plants **6**:1167-1178.
712 **Yang, Z., Wang, J., Huang, Y., Wang, S., Wei, L., Liu, D., Weng, Y., Xiang, J., Zhu,**
713 **Q., Yang, Z., et al.** (2022b). CottonMD: a multi-omics database for cotton
714 biological study. Nucleic Acids Res. **51**:D1446-D1456.
715 **Yu, G., Wang, L.G., Han, Y., and He, Q.Y.** (2012). clusterProfiler: an R package for
716 comparing biological themes among gene clusters. OMICS **16**:284-287.
717 **Yu, J., Pressoir, G., Briggs, W.H., Vroh Bi, I., Yamasaki, M., Doebley, J.F.,**
718 **McMullen, M.D., Gaut, B.S., Nielsen, D.M., Holland, J.B., et al.** (2006). A
719 unified mixed-model method for association mapping that accounts for multiple
720 levels of relatedness. Nat. Genet. **38**:203-208.
721 **Zhang, G., Zhou, J., Peng, Y., Tan, Z., Li, L., Yu, L., Jin, C., Fang, S., Lu, S., Guo,**
722 **L., et al.** (2021). Genome-wide association studies of salt tolerance at seed
723 germination and seedling stages in *Brassica napus*. Front. Plant Sci. **12**:772708.
724 **Zhang, G., Peng, Y., Zhou, J., Tan, Z., Jin, C., Fang, S., Zhong, S., Jin, C., Wang,**
725 **R., Wen, X., et al.** (2022a). Genome-wide association studies of salt-alkali
726 tolerance at seedling and mature stages in *Brassica napus*. Front. Plant Sci.
727 **13**:857149.
728 **Zhang, Y., Zhang, H., Zhao, H., Xia, Y., Zheng, X., Fan, R., Tan, Z., Duan, C., Fu,**
729 **Y., Li, L., et al.** (2022b). Multi-omics analysis dissects the genetic architecture of
730 seed coat content in *Brassica napus*. Genome Biol. **23**:86.
731 **Zhou, X., and Stephens, M.** (2012). Genome-wide efficient mixed-model analysis for
732 association studies. Nat. Genet. **44**:821-824.
733 **Zhu, Z., Zhang, F., Hu, H., Bakshi, A., Robinson, M.R., Powell, J.E., Montgomery,**
734 **G.W., Goddard, M.E., Wray, N.R., Visscher, P.M., et al.** (2016). Integration of
735 summary data from GWAS and eQTL studies predicts complex trait gene targets.
736 Nat. Genet. **48**:481-487.
737

Supplemental information

Supplementary Figures

Supplementary Figure 1: Mining the genes associated with SOC using GWAS module.

Supplementary Tables

Supplementary Table 1: Data source of 29 genome assemblies in the Genome portal.

Supplementary Table S2: Summary of transcriptome datasets in BnIR.

Supplementary Table S3: Summary of phenotypic datasets in BnIR.

Supplementary Table S4: Summary of epigenetics datasets in BnIR.

Supplementary Table S5: Significant GWAS loci associated with traits.

Supplementary Table S6: Summary of eQTL mapping.

Supplementary Table S7: Significant genes associated with traits by TWAS.

Supplementary Table S8: Significant genes associated with traits by SMR.

Supplementary Table S9: Significant genes associated with traits by co-localization analysis.

755 # Figure legends

756 **Figure 1 Construction pipelines and overview of BnIR.**

757 **Figure 2 Integration of multi-omics data. (A)** Pipeline of integrating population-level
758 multi-omics datasets. **(B-E)** Usage of the GWAS module. **(B)** Pipeline of searching the
759 GWAS signals of seed erucic acid content. **(C)** Global GWAS signals of seed erucic
760 acid content. **(D)** List of significant variations in A08:18500000–19000000. **(E)** Local
761 Manhattan plot of A08:18500000-19000000. Purple diamond represents the lead
762 variation. Green to red dots indicate weak to strong linkage disequilibrium coefficients
763 with the lead variation. **(F-H)** Usage of eQTL module. **(F)** Pipeline of searching the
764 eQTL signals of *BnaA09.ARF18*. **(G)** List of eSNPs of *BnaA09.ARF18*. **(H)** Circos plot
765 of the global eQTLs of *BnaA09.ARF18*. Purple dot in the outer circle represents the
766 genomic position of *BnaA09.ARF18*. Purple dots in the median circle represent the P-
767 values of eSNPs. Yellow lines represent the associations between eSNPs and
768 *BnaA09.ARF18*.

769 **Figure 3 Multi-omics tools in the Tools portal of BnIR.** A total of 18 tools were
770 integrated into the Tools portal, including Jbrowse **(A)**, BLAST **(B)**, MSA **(C)**, GO
771 enrichment analysis **(D)**, KEGG enrichment analysis **(E)**, co-localization analysis
772 (COLOC) **(F)**, SMR **(G)**, germplasm identification tool SNPmatch **(H)**, primer design
773 tool Primer3 **(I)** and electronic PCR tool e-PCR **(J)**.

774 **Figure 4 Case study of mining the genes associated with SGC. (A)** Pipeline of
775 searching SGC in GWAS module. **(B)** Genome-wide Manhattan plot of SGC in the
776 GWAS module. **(C)** List of 402 significant variations associated with SGC identified
777 by GWAS. **(D)** Local Manhattan plot of SGC at C09: 4.0–4.5 Mb. Two purple texts
778 represent *BnaC09.MYB28a* and *BnaC09.MYB28b*. **(E)** Pipeline of searching the co-
779 localization analysis results of *BnaC09.MYB28*s in BnIR. **(F-G)** Co-localization
780 analysis of *cis*-eQTLs of two *BnaC09.MYB28*s and GWAS loci. *Cis*-eQTL signals of
781 *BnaC09.MYB28a* **(F)** and *BnaC09.MYB28b* **(G)** co-localized with the *qGLS.C09.8*
782 locus in GWAS. In **(D)**, **(F)** and **(G)**, purple diamonds represent the lead variations (one

783 4-bp frameshift InDel of GCTA/-), and green to red dots indicate weak to strong linkage
784 disequilibrium coefficients with the lead variation.

785 **Figure 5 Case study of identifying new genes associated with SOC. (A)** Pipeline of
786 searching the co-localization analysis results of *BnaC07.SnRK2D* in BnIR. **(B-D)** Co-
787 localization analysis of *cis*-eQTL of *BnaC07.SnRK2D* and GWAS loci. **(B-C)** Local
788 Manhattan plots of SOC in GWAS **(B)** and *BnaC07.SnRK2D* in eQTL mapping **(C)**.
789 **(D)** *Cis*-eQTL signals of *BnaC07.SnRK2D* co-localized with *qOC.C07.1* locus in
790 GWAS. Purple diamond represents the lead variation. Green to red dots indicate weak
791 to strong linkage disequilibrium coefficients with the lead variation. **(E)** Pipeline of
792 searching variations in *BnaC07.SnRK2D* using the Single-locus module. **(F)** Variations
793 in *BnaC07.SnRK2D* and its upstream and downstream variation within 1 kb. Red,
794 orange, blue and black inverted triangles represent variations with high, moderate, low
795 and modifier effects. Pink dots represent significant variations with SOC in GWAS. **(G)**
796 Pipeline of haplotype analysis using the Multi-locus module. **(H-I)** Violin plots of SOC
797 **(H)** and expression levels of *BnaC07.SnRK2D* **(I)** in accessions with Hap1 (orange
798 boxes) and Hap2 (blue boxes).

799 **Figure 6 New features of BnIR. (A)** Upgrade of BnIR relative to BnPIR, BnTIR and
800 BnVIR. Red bold texts represent new datasets in BnIR. **(B)** Comparison of BnIR with
801 other *B. napus* omics databases. Green to yellow cells represent fewer to more omics
802 datasets.

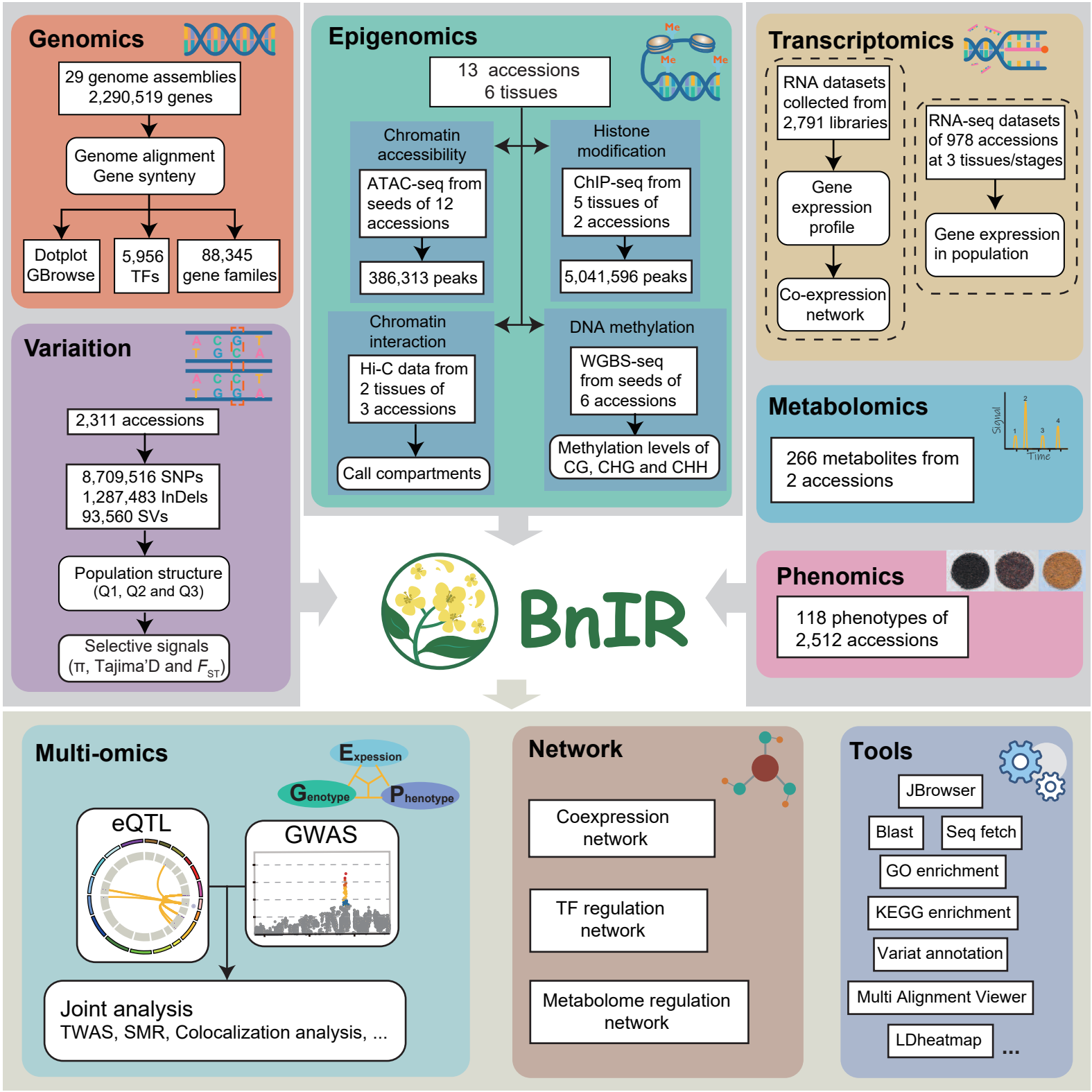
Genomics
29 genome assemblies
2,290,519 genes
Genome alignment
Gene synteny
Dotplot
GBrowse
5,956
TFs
88,345
gene familes
Variaition
2,311 accessions
8,709,516 SNPs
1,287,483 InDels
93,560 SVs
Population structure
(Q1, Q2 and Q3)
Selective signals
(π, Tajima'D and F_{ST})
Epigenomics
13 accessions
6 tissues
Chromatin accessibility
ATAC-seq from seeds of 12 accessions
386,313 peaks
Histone modification
ChIP-seq from 5 tissues of 2 accessions
5,041,596 peaks
Chromatin interaction
Hi-C data from 2 tissues of 3 accessions
Call compartments
DNA methylation
WGBS-seq from seeds of 6 accessions
Methylation levels of CG, CHG and CHH
Transcriptomics
RNA datasets collected from 2,791 libraries
Gene expression profile
Co-expression network
RNA-seq datasets of 978 accessions at 3 tissues/stages
Gene expression in population
Metabolomics
266 metabolites from 2 accessions
Signal
Time
Phenomics
118 phenotypes of 2,512 accessions
BnIR
Multi-omics
Expression
Genotype
Phenotype
eQTL
GWAS
Joint analysis
TWAS, SMR, Colocalization analysis, ...
Network
Coexpression network
TF regulation network
Metabolome regulation network
Tools
JBrowser
Blast
Seq fetch
GO enrichment
KEGG enrichment
Variat annotation
Multi Alignment Viewer
LDheatmap
...

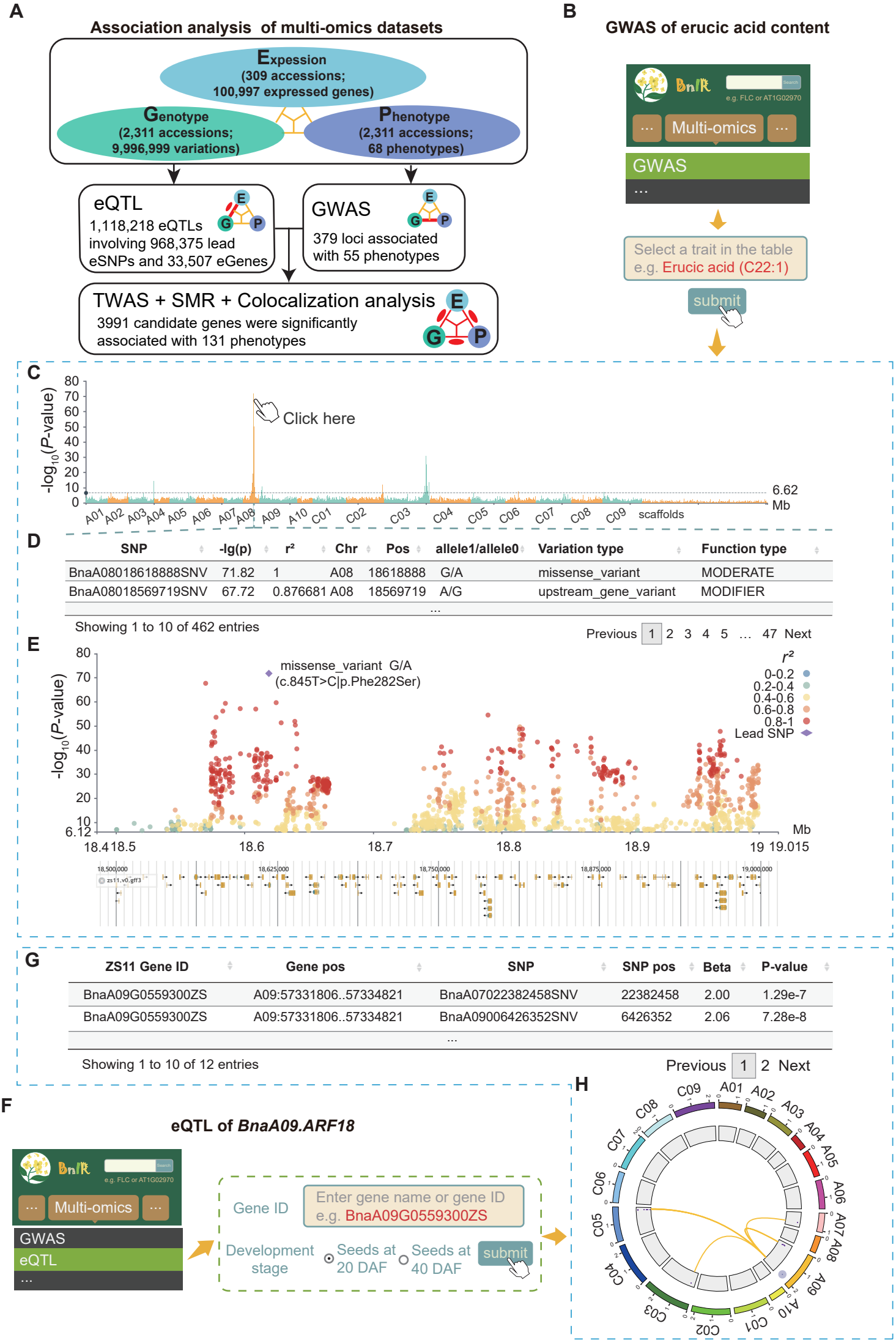
A
Association analysis of multi-omics datasets
Expression
(309 accessions;
100,997 expressed genes)
Genotype
(2,311 accessions;
9,996,999 variations)
Phenotype
(2,311 accessions;
68 phenotypes)
eQTL
1,118,218 eQTLs
involving 968,375 lead
eSNPs and 33,507 eGenes
GWAS
379 loci associated
with 55 phenotypes
TWAS + SMR + Colocalization analysis
3991 candidate genes were significantly
associated with 131 phenotypes
B
GWAS of erucic acid content
e.g. FLC or AT1G02970
Multi-omics
GWAS
...
Select a trait in the table
e.g. Erucic acid (C22:1)
submit
C
-log10(P-value)
Click here
6.62
Mb
A01 A02 A03 A04 A05 A06 A07 A08 A09 A10 C01 C02 C03 C04 C05 C06 C07 C08 C09 scaffolds
D
SNP | -lg(p) | r² | Chr | Pos | allele1/allele0 | Variation type | Function type
BnaA08018618888SNV | 71.82 | 1 | A08 | 18618888 | G/A | missense_variant | MODERATE
BnaA08018569719SNV | 67.72 | 0.876681 | A08 | 18569719 | A/G | upstream_gene_variant | MODIFIER
...
Showing 1 to 10 of 462 entries
Previous 1 2 3 4 5 ... 47 Next
E
missense_variant G/A
(c.845T>C|p.Phe282Ser)
r²
0-0.2
0.2-0.4
0.4-0.6
0.6-0.8
0.8-1
Lead SNP
6.12
18.4 18.5 18.6 18.7 18.8 18.9 19 19.015
Mb
G
ZS11 Gene ID | Gene pos | SNP | SNP pos | Beta | P-value
BnaA09G0559300ZS | A09:57331806..57334821 | BnaA07022382458SNV | 22382458 | 2.00 | 1.29e-7
BnaA09G0559300ZS | A09:57331806..57334821 | BnaA09006426352SNV | 6426352 | 2.06 | 7.28e-8
...
Showing 1 to 10 of 12 entries
Previous 1 2 Next
F
eQTL of BnaA09.ARF18
Multi-omics
GWAS
eQTL
...
Gene ID
Enter gene name or gene ID
e.g. BnaA09G0559300ZS
Development stage
Seeds at 20 DAF
Seeds at 40 DAF
submit
H
A01 A02 A03 A04 A05 A06 A07 A08 A09 A10 C01 C02 C03 C04 C05 C06 C07 C08 C09

Tools

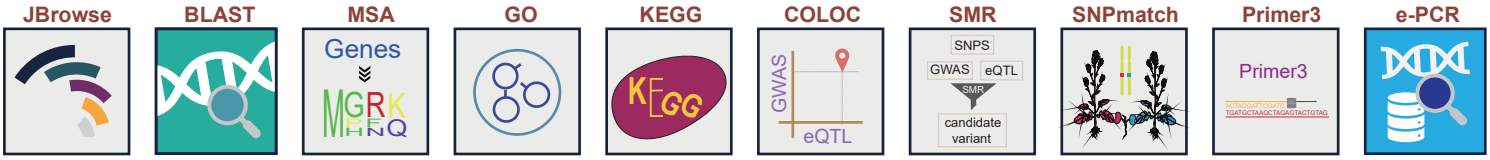

Seq fetch, Heatmap, LDheatmap, Data2geomap, Data2heatmap, Domain search, ...

A

B

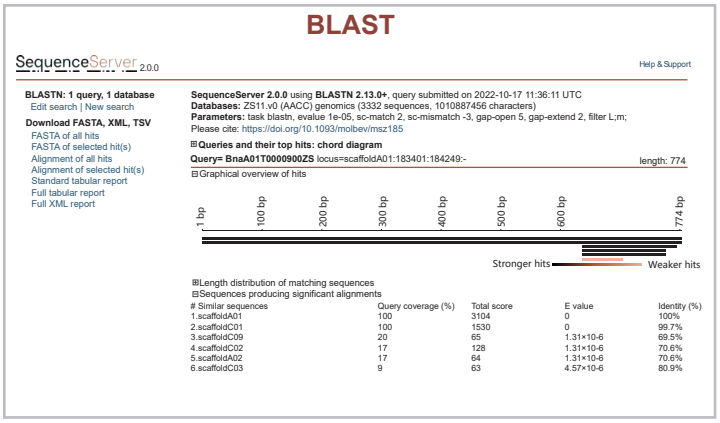

C

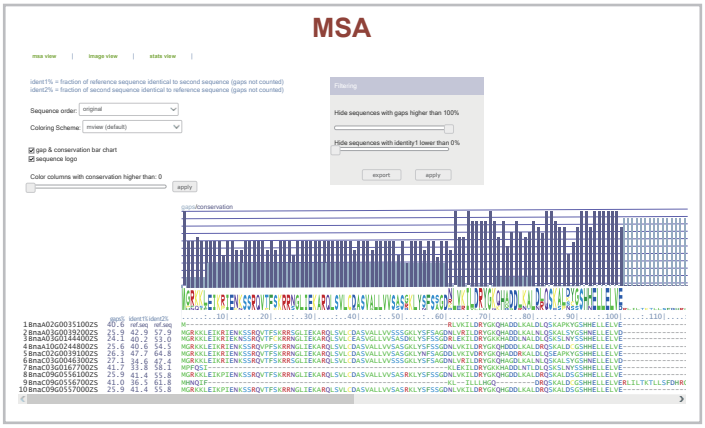

D

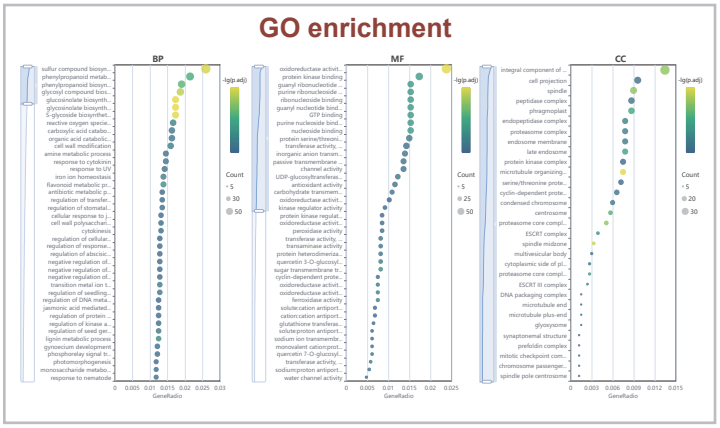

E

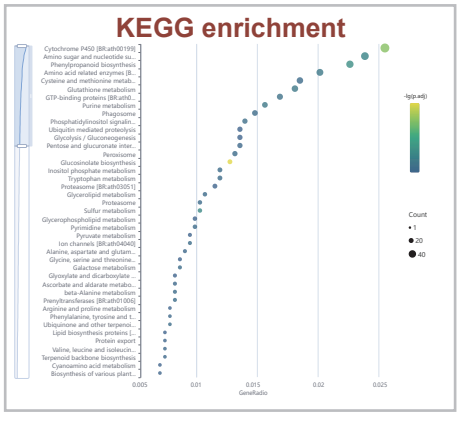

F

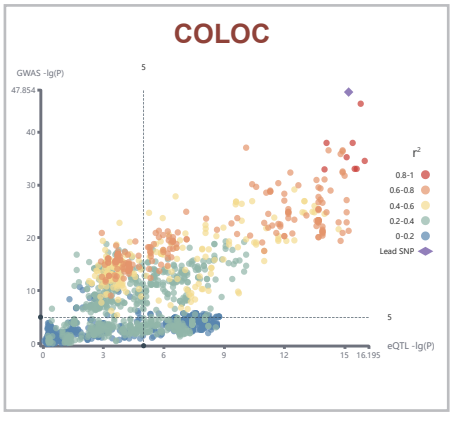

G

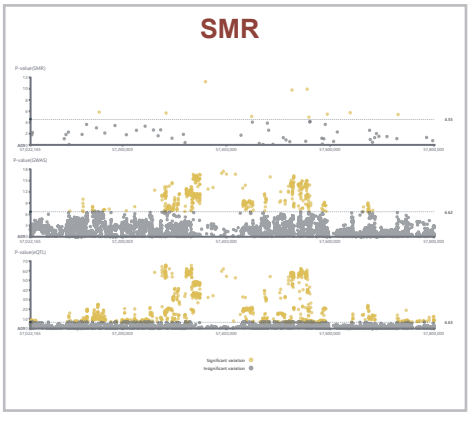

H

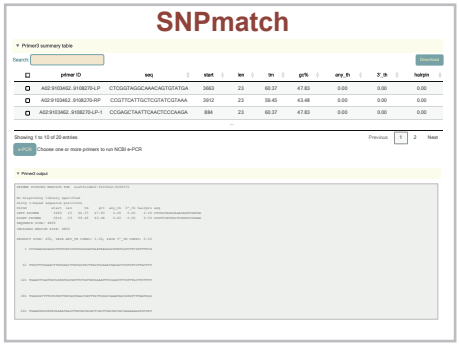

I

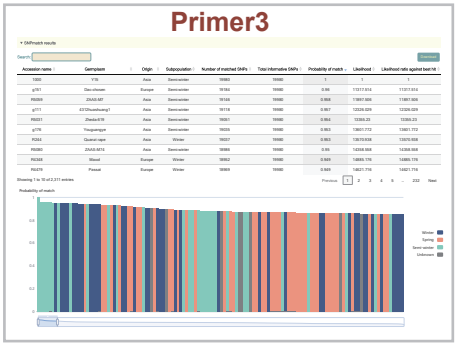

J

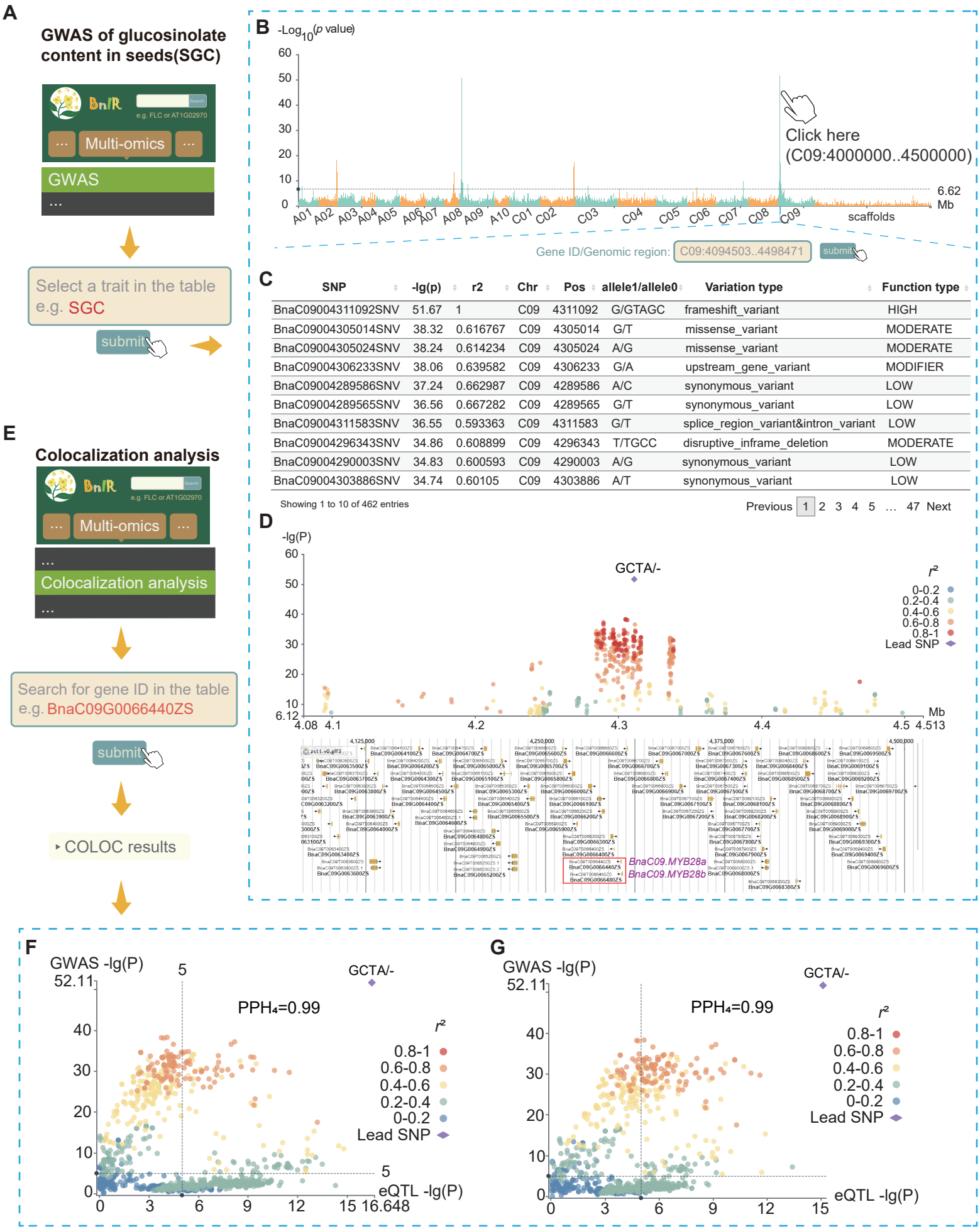
A
GWAS of glucosinolate content in seeds(SGC)
BnIR
e.g. FLC or AT1G02970
Multi-omics
GWAS
Select a trait in the table
e.g. SGC
submit
B
-Log10(p value)
Click here
(C09:4000000..4500000)
6.62
Mb
scaffolds
Gene ID/Genomic region: C09:4094503..4498471
submit
C
SNP | -lg(p) | r2 | Chr | Pos | allele1/allele0 | Variation type | Function type
BnaC09004311092SNV | 51.67 | 1 | C09 | 4311092 | G/GTAGC | frameshift_variant | HIGH
BnaC09004305014SNV | 38.32 | 0.616767 | C09 | 4305014 | G/T | missense_variant | MODERATE
BnaC09004305024SNV | 38.24 | 0.614234 | C09 | 4305024 | A/G | missense_variant | MODERATE
BnaC09004306233SNV | 38.06 | 0.639582 | C09 | 4306233 | G/A | upstream_gene_variant | MODIFIER
BnaC09004289586SNV | 37.24 | 0.662987 | C09 | 4289586 | A/C | synonymous_variant | LOW
BnaC09004289565SNV | 36.56 | 0.667282 | C09 | 4289565 | G/T | synonymous_variant | LOW
BnaC09004311583SNV | 36.55 | 0.593363 | C09 | 4311583 | G/T | splice_region_variant&intron_variant | LOW
BnaC09004296343SNV | 34.86 | 0.608899 | C09 | 4296343 | T/TGCC | disruptive_inframe_deletion | MODERATE
BnaC09004290003SNV | 34.83 | 0.600593 | C09 | 4290003 | A/G | synonymous_variant | LOW
BnaC09004303886SNV | 34.74 | 0.60105 | C09 | 4303886 | A/T | synonymous_variant | LOW
Showing 1 to 10 of 462 entries
Previous 1 2 3 4 5 … 47 Next
D
-lg(P)
GCTA/-
r²
0-0.2
0.2-0.4
0.4-0.6
0.6-0.8
0.8-1
Lead SNP
6.12
4.08 4.1 4.2 4.3 4.4 4.5 4.513
Mb
BnaC09.MYB28a
BnaC09.MYB28b
E
Colocalization analysis
Colocalization analysis
Search for gene ID in the table
e.g. BnaC09G0066440ZS
submit
COLOC results
F
GWAS -lg(P)
52.11
5
GCTA/-
PPH4=0.99
r²
0.8-1
0.6-0.8
0.4-0.6
0.2-0.4
0-0.2
Lead SNP
5
eQTL -lg(P)
0 3 6 9 12 15 16.648
G
GWAS -lg(P)
52.11
GCTA/-
PPH4=0.99
r²
0.8-1
0.6-0.8
0.4-0.6
0.2-0.4
0-0.2
Lead SNP
eQTL -lg(P)
0 3 6 9 12 15

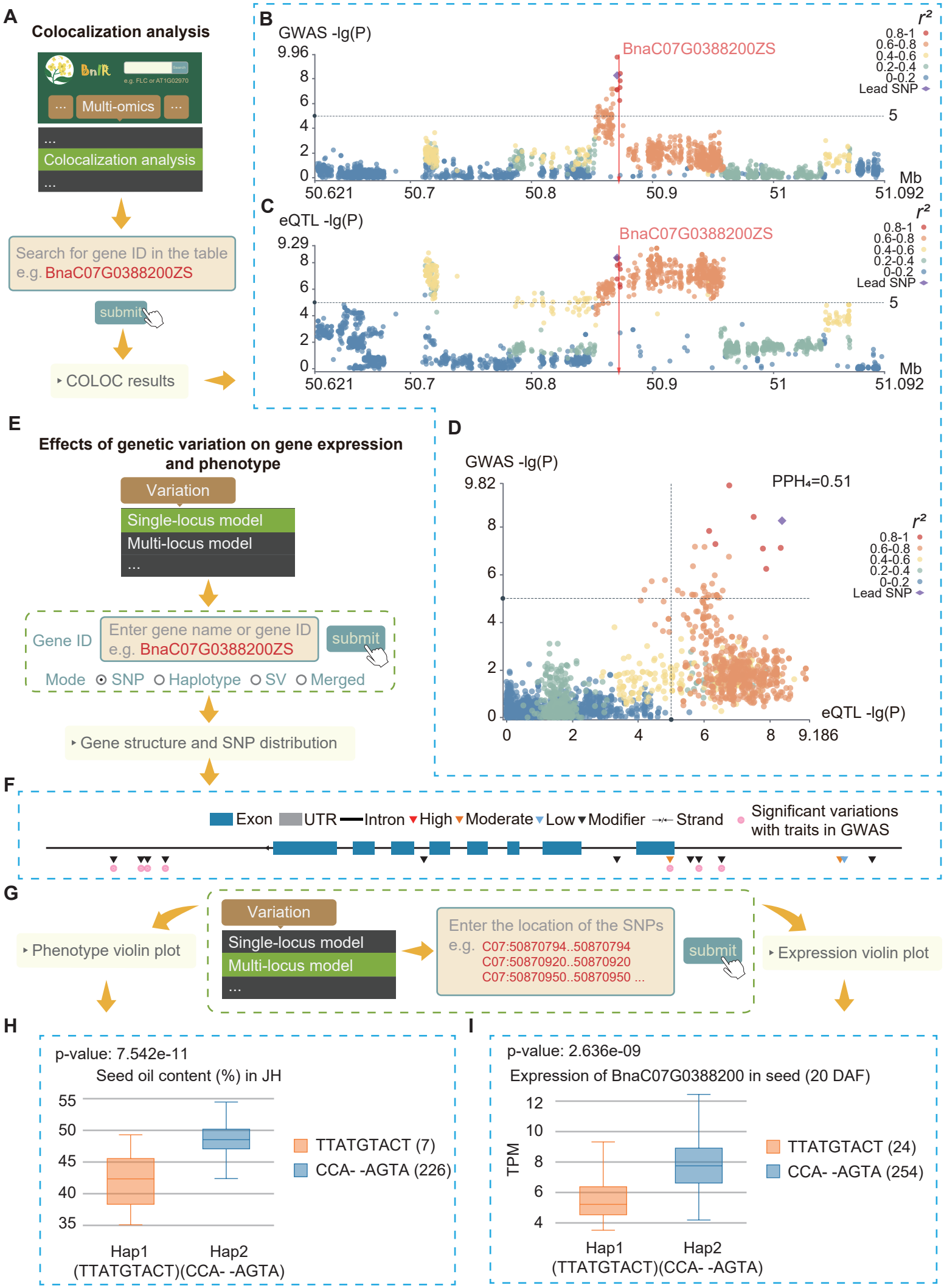
A
Colocalization analysis
BnIR
e.g. FLC or AT1G02970
Multi-omics
Colocalization analysis
Search for gene ID in the table
e.g. BnaC07G0388200ZS
submit
COLOC results
B
GWAS -lg(P)
BnaC07G0388200ZS
r²
0.8-1
0.6-0.8
0.4-0.6
0.2-0.4
0-0.2
Lead SNP
Mb
50.621
50.7
50.8
50.9
51
51.092
C
eQTL -lg(P)
BnaC07G0388200ZS
E
Effects of genetic variation on gene expression and phenotype
Variation
Single-locus model
Multi-locus model
Gene ID
Enter gene name or gene ID
e.g. BnaC07G0388200ZS
submit
Mode
SNP
Haplotype
SV
Merged
Gene structure and SNP distribution
D
GWAS -lg(P)
PPH4=0.51
eQTL -lg(P)
9.186
F
Exon
UTR
Intron
High
Moderate
Low
Modifier
Strand
Significant variations with traits in GWAS
G
Phenotype violin plot
Variation
Single-locus model
Multi-locus model
Enter the location of the SNPs
e.g. C07:50870794..50870794
C07:50870920..50870920
C07:50870950..50870950 ...
submit
Expression violin plot
H
p-value: 7.542e-11
Seed oil content (%) in JH
TTATGTACT (7)
CCA- -AGTA (226)
Hap1
(TTATGTACT)
Hap2
(CCA- -AGTA)
I
p-value: 2.636e-09
Expression of BnaC07G0388200 in seed (20 DAF)
TPM
TTATGTACT (24)
CCA- -AGTA (254)
Hap1
(TTATGTACT)
Hap2
(CCA- -AGTA)

A

Upgrade and integration of BnPIR, BnTIR and BnVIR

Data source	BnIR		
	Portal	**New dataset**	**Improved function**
BnPIR 9 genome assemblies	Genome	+**20** genome assemblies. Totally, **2,290,519** genes; **88,423** gene index; **21,508** gene clusters; **179** gene families; **58** TF families	Optimized user experience and response speed New funciton: Gene search, Gene family, Gene cluster, Transcription factor.
BnTIR 91 RNA-seq libraries	Transcriptome	+**2,700** RNA-seq libraries, including **192** from ZS11 at 7 hormone treatments, **345** from ZS11 at 6 abiotic stress treatments and **978** from population-level assessions of 3 tissues and **1,185** from other studies	Greatly impoved response speed of eFP (**9.348 s** to **0.0611 s)** New funciton: Meta-library, Population expression, eFP (multi-gene module).
BnVIR 2,311 accessions 10,090,561 variations 21 phenotypes	Population, Variation, Phenotype, Multiomics	+**97** phenotypes of **2,512** accessions	New funciton: Phenotype search, eQTL, TWAS, SMR, Colocalization analysis.

New Portal	New dataset	Function description
Epigenome	**99** ChIP-seq libraries; **8** ATAC-seq libraries; **12** WGBS-seq libraries; **3** Hi-C libraries	Searching the peaks of ChIP-seq and ATAC-seq, the CG, CHG and CHH methylation levels, Hi-C contact frequencies and features; Browse epigenetic signals in Jbrowser
Metabolome	**266** metabolites of **2** accessions	Searching meyabolite contents
Multiomics	GWAS, eQTL, TWAS, SMR and colocalization analysis results using **55** phenotypes of **2,311** accessions	Browse the signals of GWAS, eQTL, TWAS, SMR and colocalization analysis results

B

Comparison of BnIR with the published *B. napus* database

Database	Major function
BnIR	Genome information, gene expression, epigenetic signal, metabolite content, traits, multi-omics association information, analysis and visualization tools.
BrassicaEDB	Comprehensive gene expression profile information and a user-friendly visualization interface.
BnaSNPDB	An interactive web-based platform and set of analytic tools for effcient retrieve and analysis of SNPs among 1,007 accessions.
BnaGVD	A large number of variations and search tools for accelerating studies on the functional genomics and the screening of molecular markers.

Database	Genome	Transcriptome (meta-library)	Transcriptome (population)	Epigenome	Variation	Phenotype	Metabolome
Unit	genome assemblies	libraries	libraries	libraries	accessions	phenotypes	metabolites
BnIR	**29**	**2,791**	**978**	**128**	**2,311**	**118**	**544**
BrassicaEDB	**1**	**837**	-	-	-	-	-
BnaSNPDB	-	-	-	-	**1,007**	-	-
BnaGVD	**3**	-	-	-	**1,007**	**10**	-

Database	Variation-Phenotype	Variation-Expression	Network analysis	Association analysis
BnIR	√	√	√	**GWAS, eQTL, TWAS, SMR, colocalization analysis**
BrassicaEDB	-	-	-	-
BnaSNPDB	-	-	-	-
BnaGVD	-	-	-	**GWAS**

Supplemental information

BnIR: a multi-omics database with various tools for *Brassica napus* research and breeding

Zhiquan Yang[1,2,3,†], Shengbo Wang[1,2,†], Lulu Wei[1,2], Yiming Huang[1,2], Dongxu Liu[1,2], Yupeng Jia[1,2], Chengfang Luo[1,2], Yuchen Lin[1,2], Congyuan Liang[1,2], Yue Hu[1,2], Cheng Dai[1], Liang Guo[1], Yongming Zhou[1], Qing-Yong Yang[1,2,*]

[1]National Key Laboratory of Crop Genetic Improvement, Hubei Hongshan Laboratory, Huazhong Agricultural University, Wuhan, 430070, China

[2]Hubei Key Laboratory of Agricultural Bioinformatics, College of Informatics, Huazhong Agricultural University, Wuhan, 430070, China

[3]Innovative Center of Molecular Genetics and Evolution, School of Life Sciences, Guangzhou University, Guangzhou, 510405, China

[†]These authors contributed equally: Zhiquan Yang, Shengbo Wang.

[*]Correspondence: Qing-Yong Yang (email: yqy@mail.hzau.edu.cn)

A **GWAS of glucosinolate content in seeds(SGC)**

B

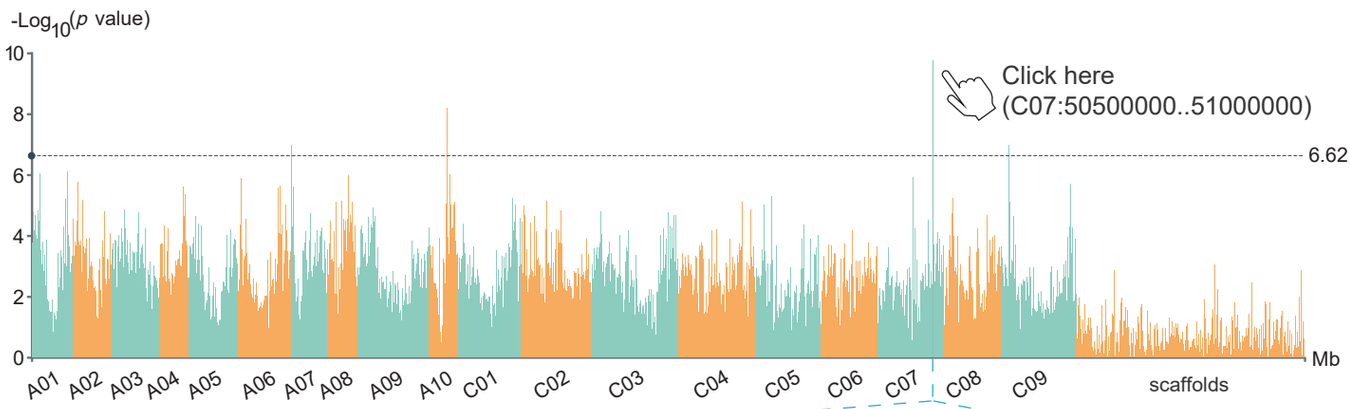

Gene ID/Genomic region: C07:50500000..51000000 submit

C

SNP	-lg(GWAS_p)	LD_r2 (to lead SNP)	PVE(r2)	Beta	SE	Chr	Pos	allele1/allele0	Variation type	Function type
BnaC07050870920SNV	9.74	1.0000	0.0958	-2.661518	0.4021322	C07	50870920	T/C	upstream_gene_variant	MODIFIER
BnaC07050871032SNV	7.09	0.9411	0.0716	-2.30125	0.4176682	C07	50871032	T/A	upstream_gene_variant	MODIFIER
BnaC07050870950SNV	8.26	0.9406	0.0785	-2.422521	0.4024712	C07	50870950	ATG/A	upstream_gene_variant	MODIFIER
BnaC07050870794SNV	7.12	0.9292	0.0667	-2.220025	0.4018871	C07	50870794	T/C	upstream_gene_variant	MODIFIER
BnaC07050873484SNV	7.83	0.8171	0.0800	-2.445226	0.4189096	C07	50873484	C/T	upstream_gene_variant	MODIFIER
BnaC07050873588SNV	8.42	0.7994	0.0801	-2.586631	0.4252047	C07	50873588	T/A	upstream_gene_variant	MODIFIER
BnaC07050873351SNV	7.28	0.7915	0.0751	-2.472915	0.4420629	C07	50873351	A/G	missense_variant	MODERATE
BnaC07050866327SNV	7.16	0.7075	0.0710	-2.290309	0.4132066	C07	50866327	G/A	downstream_gene_variant	MODIFIER
BnaC07050867789SNV	7.17	0.6877	0.0646	-2.082158	0.3755485	C07	50867789	A/C	synonymous_variant	LOW
BnaC07050866990SNV	6.75	0.6759	0.0655	-2.152067	0.4016859	C07	50866990	A/C	downstream_gene_variant	MODIFIER

Showing 1 to 10 of 10 entries

Previous 1 Next

D

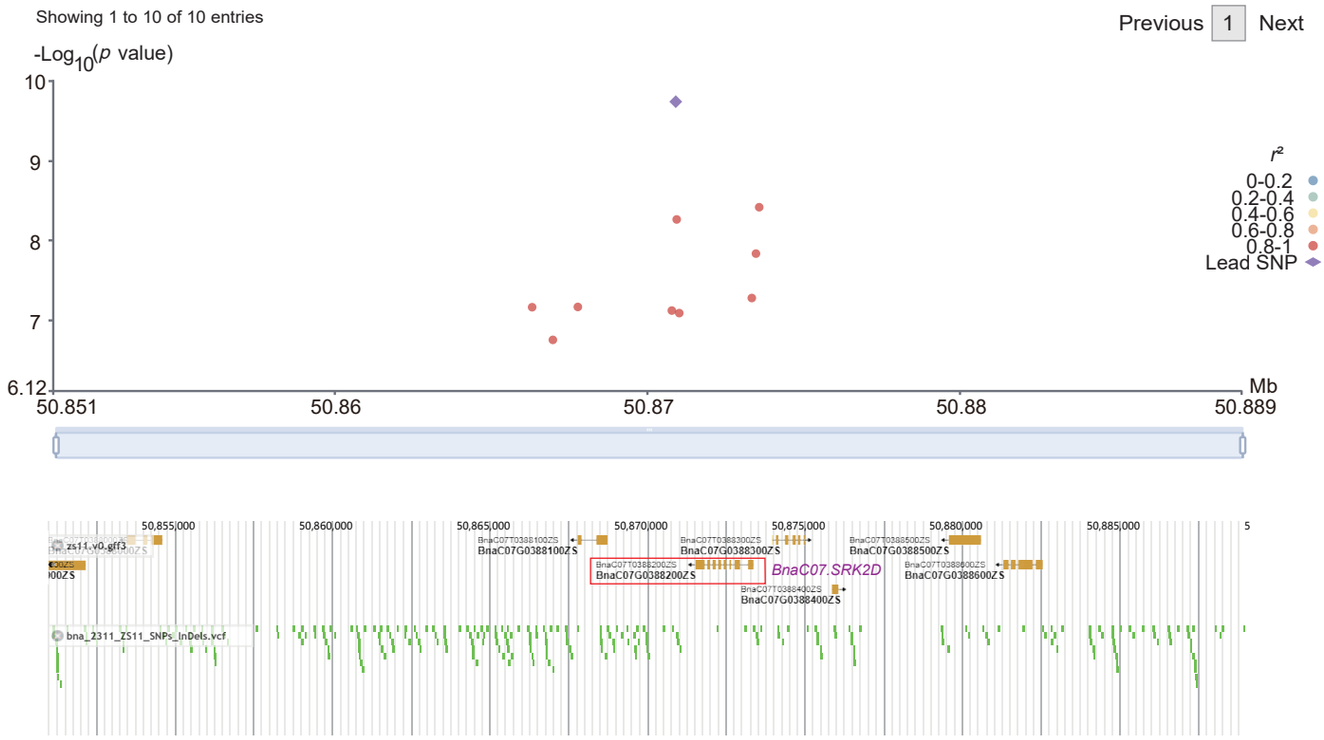

Supplementary Figure 1: Mining the genes associated with SOC using GWAS module. (A) Pipeline of searching SOC in GWAS module. **(B)** Genome-wide Manhattan plot of SOC in the GWAS module. **(C)** List of 10 significant variations associated with SOC identified by GWAS. **(D)** Local Manhattan plot of SOC at C07: 50.5–51.0 Mb. The purple text represents *BnaC07.SRK2D*.